

2-Port High Gain Millimeter-Wave MIMO Antenna for 5G Applications

Ming Ming Gao, Hong Liang Niu*, Jing Chang Nan, Wen Hui Liu, and Chun Li Liu

Abstract—In order to improve the distance of 5th Generation (5G) Mobile Communication Technology) millimeter-wave outdoor point-to-point relay transmission, a 2-port Multiple Input Multiple Output (MIMO) antenna with high gain and low sidelobe level characteristics is designed at 39 GHz. The antenna is designed using the Taylor synthesis method and slotting technology to increase the antenna gain and lower the sidelobe level. Loading hollow T-shaped branches reduces the mutual coupling between MIMO antennas. The measured results are basically in line with the simulation ones. The results show that the bandwidth of the antenna is 38.1 ~ 39.3 GHz; the isolation degree is more than 50 dB; the antenna gain is 25.75 dBi at 39 GHz; the *E*-plane and *H*-plane sidelobe levels are -20.5 dB and -20 dB, respectively. Furthermore, the Envelope Correlation Coefficient (ECC) is less than 0.022; the Diversity Gain (DG) is more than 9.89; and the radiation efficiency reaches 90% in the working frequency band. Therefore, this antenna can be used as a long-distance relay antenna in 5G millimeter-wave communication system with high gain and low sidelobe level characteristics based on meeting the requirements of the MIMO antenna.

1. INTRODUCTION

Nowadays, 5G has become a hotspot in wireless communication [1], and in 2016 the Federal Communications Commission of the United States assigned the 28 GHz, 37 GHz, and 39 GHz bands in the millimeter-wave band to 5G operations. Among them, 39 GHz millimeter-wave does not have much extra attenuation in atmospheric propagation, and the radio wave propagation only fades about 80% beyond the cell coverage radius of 200 m in lousy weather conditions [2], which makes 39 GHz millimeter-wave communication highly utilized. In wireless communication, relay antennas significantly improve the transmission distance of electromagnetic waves. At the same time, to improve the efficiency and reliability of electromagnetic wave transmission, most relay antennas introduce the multiple-input multiple-output (MIMO) technology [3–5]. MIMO technology has been widely used. Ref. [6] designed a compact ultra-wideband MIMO antenna. Ref. [7] designed a defected ground structure (DGS)-based miniaturized MIMO antenna. Ref. [8] designed a dual-band millimeter-wave MIMO antenna. However, these MIMO antennas do not have high gain, which is critical to the communication distance [9]. In order to avoid the influence of clutter on the antenna performance during long-distance communication, it is necessary to increase the antenna gain and reduce the antenna sidelobe level. There are many methods to realize high gain and low sidelobe level, such as changing the feed power ratio of the array element [10] and loading Complementary split-ring resonant (CSRR) structure [11]. However, the array antenna does not have the performance of MIMO antenna transceiver integration. Therefore, using a high gain MIMO antenna as a long-distance relay antenna is a good choice. High gain MIMO antennas have been the subject of design and research by scholars. Ref. [12] designed a four-port high gain MIMO antenna applied to a 5G millimeter-wave communication system with a resonance frequency of 28 GHz

Received 7 August 2023, Accepted 30 September 2023, Scheduled 14 October 2023

* Corresponding author: Hongliang Niu (1356443071@qq.com).

The authors are with the School of Electronic and Information Engineering, Liaoning Technical University, Huludao 125105, China.

and a gain of 8.3 dBi. Ref. [13] designed a high gain MIMO antenna applied to 5G millimeter-wave intelligent devices with a resonance frequency of 41 GHz and a gain of 9.86 dBi. Ref. [14] designed a millimeter-wave high gain MIMO antenna at 37 GHz, which increased the gain to 12.8 dBi while satisfying the MIMO performance. However, due to insufficient gain, most of the existing high-gain MIMO antennas are unsuitable for long-distance wireless relaying.

The above antennas cannot meet the requirements of long-distance communication. In order to solve the above problems, this paper designs a MIMO antenna with high gain and low sidelobe characteristics, which is suitable for outdoor long-distance point-to-point relay transmission. Firstly, an array antenna with high gain and low sidelobe characteristics is designed using the Taylor synthesis method. Secondly, a rectangular slot is etched on the ground plane to reduce the sidelobe level further. Finally, a hollow T-shaped branch is loaded between the antennas to reduce the mutual coupling. The size of the final antenna is $190.46 \times 56.65 \times 0.254 \text{ mm}^3$, and the measured bandwidth is 38.1 ~ 39.3 GHz. At 39 GHz, the antenna gain is 25.75 dBi, and the sidelobe levels of E -plane and H -plane achieve -20 dB , which meets the expected design goal. The isolation degree S_{21} is greater than 50 dB; ECC is less than 0.022; DG is greater than 9.89, which meet the design requirement of MIMO antenna.

2. DESIGN OF COMB ARRAY ANTENNA

2.1. Infrastructure

The structure of the microstrip comb array antenna is shown in Figure 1. The antenna consists of a feed line and multiple open stub lines, in which the open stub lines on both sides are radiating structures. Alternating stubs form the comb array antenna, the distance ss between adjacent stubs is $\frac{\lambda_g}{2}$, and the length ls of the stubs is also $\frac{\lambda_g}{2}$ [15]. The radiating structures of the antenna are printed on the top layer of the dielectric substrate, and the grounding plate is printed on the bottom layer. The dielectric substrate is selected from Rogers RT5880 with a thickness of 0.254 mm, a loss angle tangent of 0.0009, and a dielectric constant 2.2.

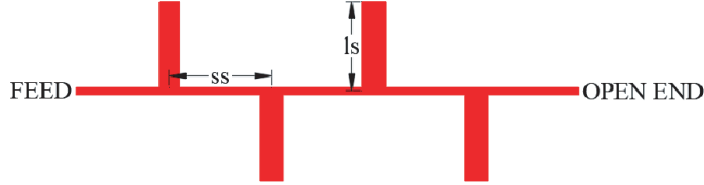


Figure 1. Basic structure of comb antenna.

2.2. Design of Comb Antenna

The Taylor synthesis method is first applied to calculate the current amplitude of each stub, followed by calculating the impedance value corresponding to each stub, and finally, obtaining the width of the stub. The following equation can express the Taylor synthesis method:

Calculate parameters R_0 , A , \bar{n} , and σ based on the preset sidelobe level $R_{0\text{dB}}$. Calculate \bar{n} using Eq. (3), where \bar{n} is the number of equal first n sidelobe levels. Calculate the lobe broadening factor σ using Eq. (4), and determine the excitation current amplitude using Eq. (5) [16].

$$R_0 = 10^{\frac{R_{0\text{dB}}}{20}} \quad (1)$$

$$A = \frac{1}{\pi} \text{arccosh} R_0 = \frac{1}{\pi} \ln \left(R_0 + \sqrt{R_0^2 - 1} \right) \quad (2)$$

$$\bar{n} \geq 2A^2 + \frac{1}{2} \quad (3)$$

$$\sigma = \frac{\bar{n}}{\sqrt{A^2 + (\bar{n} - \frac{1}{2})}} \tag{4}$$

$$I_n(Z_n) = 1 + 2 \sum_{m=1}^{\bar{n}-1} \bar{S}(m) \cos(mp), \quad n = 1, 2, \dots, N \tag{5}$$

$$\bar{S}(m) = \bar{S}(m, A, \bar{n}, \sigma) = \bar{S}(m, R_{0\text{dB}}) \tag{6}$$

The Taylor synthesis method can be directly applied to MATLAB run Taylor function to calculate the corresponding current amplitude. In this paper, the expected sidelobe level is -20 dB. To leave room for design space in actual simulation, the preset sidelobe level is -25 dB. Based on fully considering the relationship among gain, sidelobe level, size, and number of array elements, the number of array elements is selected to be 13 [15]. $\bar{n} \geq 3.08$ is calculated so that the first 4 sidelobe levels are equal in level. The current amplitude corresponding to each stub is obtained by running the Taylor function. The impedance of each stub is calculated by Eq. (7), and then the theoretical width of the truncated line is extrapolated, in which stub 1 is selected to be 0.1 mm [17], thus 129Ω . Table 1 shows the theoretical current amplitude and width of each stub.

$$Z_i = \frac{I_1 Z_1}{I_i}, \quad 2 \leq i \leq 13 \tag{7}$$

Table 1. Theoretical current amplitude and width of each stub.

Stub	Current Amplitude	Width/mm	Stub	Current Amplitude	Width/mm
1	0.5441	0.1	2	0.6532	0.17
3	0.8470	0.32	4	1.0737	0.5
5	1.2703	0.66	6	1.3943	0.75
7	1.4351	0.79	8	1.3943	0.75
9	1.2703	0.66	10	1.0737	0.5
11	0.8470	0.32	12	0.6532	0.17
13	0.5441	0.1			

Figure 2 shows the structure of the comb array antenna, with the antenna radiating structure in red and the grounding plate in cyan. CST is applied to optimize the simulation of the antenna.

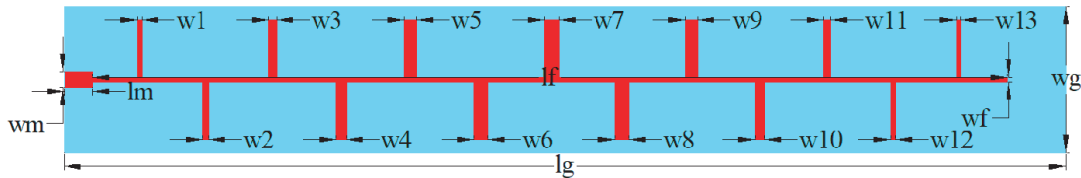


Figure 2. Comb array antenna structure.

Figure 3 shows the S_{11} simulation diagram of the antenna, from which it can be seen that the antenna’s resonant frequency varies with the change of the length ls and spacing ss of the stub. When the value of ls (ss) is specific, the resonant frequency moves to the low frequency with increased ss (ls). The red curve has a resonant frequency of 39 GHz, and the value of S_{11} reaches -50 dB. At this time, $ls = 2.667$, $ss = 3.508$ are the optimum values.

The radiation patterns diagram of the optimized comb array antenna is shown in Figure 4, from which it can be seen that the peak gain of the H -plane of the antenna is 16.9 dBi, and the sidelobe level is -22.7 dB.

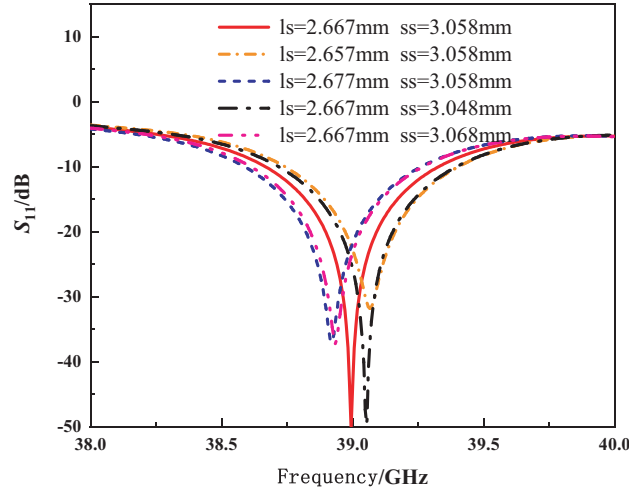


Figure 3. Antenna S_{11} parameters.

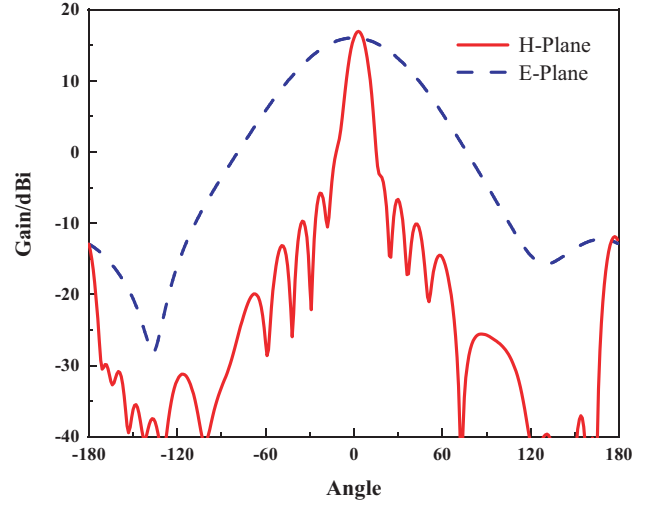


Figure 4. Radiation patterns.

3. DESIGN OF HIGH GAIN LOW SIDELOBE ARRAY ANTENNAS

3.1. Number of Elements

In order to meet the long-distance transmission, this paper takes the gain of 25 dBi as the design goal because the number of antennas doubles with every gain increase of 3 dBi, so this paper will be 16 comb array antennas which are connected in parallel to form a surface array. At the same time, the Taylor synthesis method is used to reduce the antenna's sidelobe level.

3.2. Spacing of Elements

The array antenna designed in this paper is a side-shooting array, and the condition of no gate lobes is pitch $d < \lambda$. The array antenna is further fine-tuned by combining CST based on the careful consideration of inter-array mutual coupling and array size. Using MATLAB to run the Taylor function, the current amplitudes of 16 ports are obtained, and the current amplitude of each port is shown in Table 2.

Table 2. The current amplitude of each port.

Port	Current Amplitude	Port	Current Amplitude	Port	Current Amplitude
1	0.5393	2	0.6124	3	0.7483
4	0.9244	5	1.1078	6	1.2651
7	1.3743	8	1.4284	9	1.4284
10	1.3743	11	1.2651	12	1.1078
13	0.9244	14	0.7483	15	0.6124
16	0.5393				

As shown in Figure 5, 16 arrays are formed into a face array of the unfed network, and each port is fed according to the current amplitude while the spacing of the arrays d is fine-tuned. Determine the optimal value of spacing d through simulation optimization to achieve optimal impedance matching and antenna radiation characteristics. After optimization, the spacing $d = 5.81$ mm.

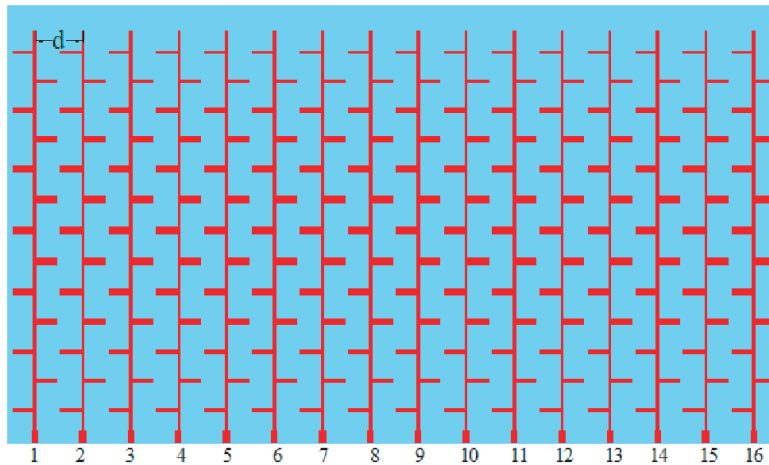


Figure 5. Array antenna without feed network.

3.3. Design of Feeder Network

To ensure that each port’s phase is consistent, each branch’s feeder length is equal. The antenna as a whole adopts a left-right symmetric structure, and the feeder network consists of 15 T-shaped power dividers, of which 7 power dividers on the left side and 7 power dividers on the right side are symmetric, and Figure 6 shows the schematic diagram of the unequal power divider with 1 input port and 16 output ports.



Figure 6. Schematic diagram of the unequal power divider with 1 input port and 16 output ports.

According to Eq. (8), the power allocation of each port in the ideal state can be derived, and the power allocation of each port is shown in Table 3. CST is applied to the unequal power divider for simulation optimization. The optimized power divider S -parameters are shown in Figure 7. It can be seen that the S -parameters of each port are very close to the calculated values, and S_{11} is below -20 dB from 38.2 GHz to 40 GHz and reaches the lowest value near 39 GHz.

$$P_i = 10 \log \frac{I_i}{I_1 + I_2 + \dots + I_i} \tag{8}$$

Table 3. Power allocation for each port.

S -parameters	Calculated value/dB	S -parameters	Calculated value/dB	S -parameters	Calculated value/dB
S_{21}	-14.72	S_{31}	-14.17	S_{41}	-13.3
S_{51}	-12.38	S_{61}	-11.59	S_{71}	-11
S_{81}	-10.66	S_{91}	-10.49	S_{101}	-10.49
S_{111}	-10.66	S_{121}	-11	S_{131}	-11.59
S_{141}	-12.38	S_{151}	-13.3	S_{161}	-14.17
S_{171}	-14.72				

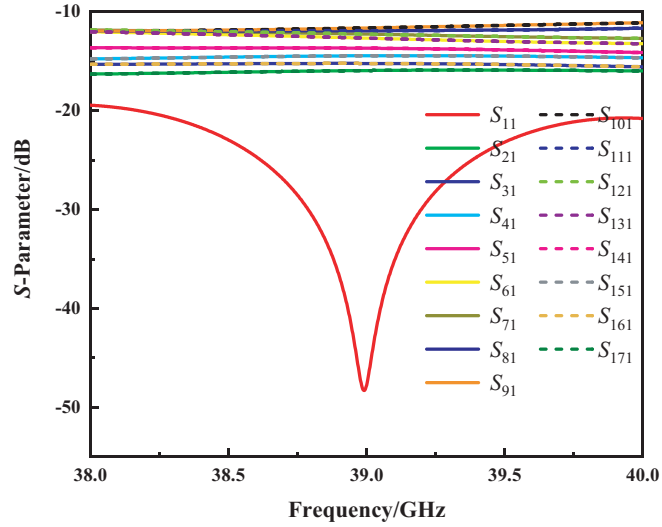


Figure 7. 1 split 16 unequal power divider S parameters.

3.4. Design of Array Antenna

Due to the close distance between the arrays, it is easy to cause the mutual coupling to affect the antenna's sidelobe level. To further reduce the sidelobe level, this article etches 15 identical rectangular slots on the ground plane, which are located between two arrays, so that the ground planes of adjacent arrays are discontinuous, thereby reducing the impact of mutual coupling of arrays on sidelobe level, optimized by the CST simulation of the final array antenna structure as shown in Figure 8, which is yellow for the grounding plate on the rectangular slots. The length of the rectangular slot is 48 mm, and the width is 0.1 mm. The width of the antenna $W = 95.23$ mm, length $L = 56.65$ mm.

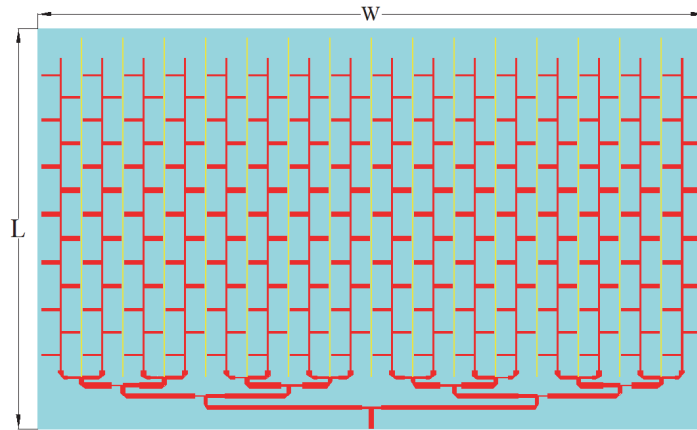


Figure 8. Final array antenna structure.

Figure 9 shows the S_{11} simulation of the final array antenna obtained after optimization by CST simulation, from which it can be seen that the resonance frequency of the antenna is 39 GHz; the S_{11} value reaches -40 dB; and the bandwidth is 38.28 GHz \sim 39.9 GHz.

Figure 10 demonstrates the comparison of the radiation direction maps without and with slots, from which it can be seen that the peak gains of the E -plane and H -plane are unchanged after the etching of the slots, and the sidelobe levels are reduced by 2 dB and 0.9 dB, respectively, when the sidelobe levels reach -22.6 dB and -22.3 dB, respectively.

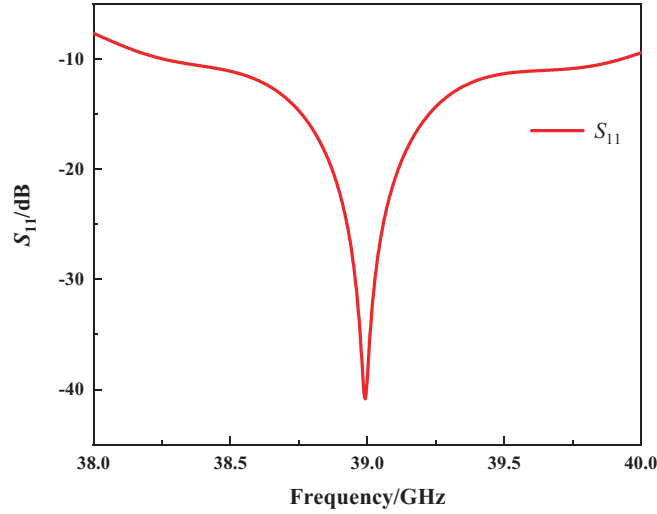


Figure 9. Array antenna S_{11} parameters.

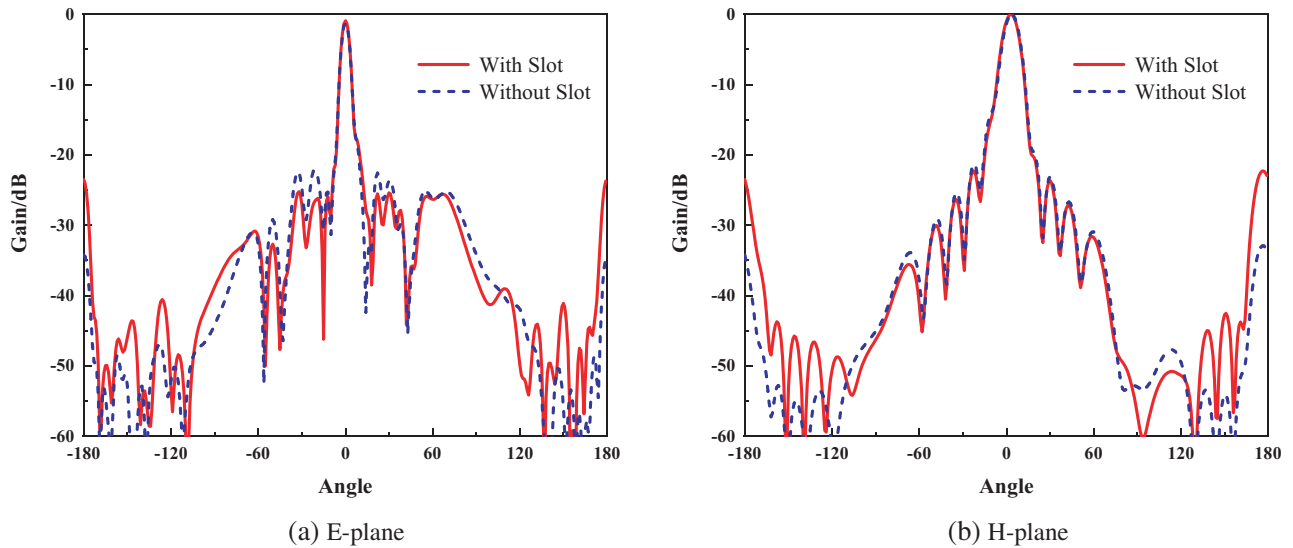


Figure 10. Comparison of Radiation pattern.

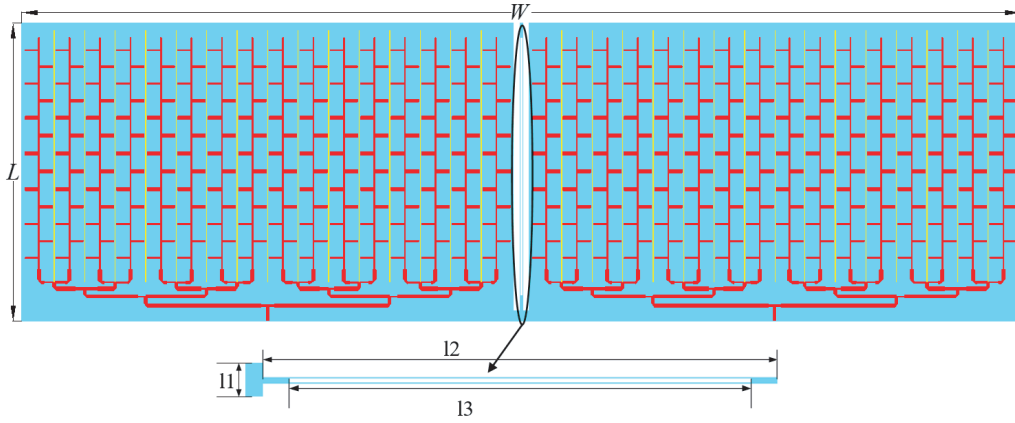
4. DESIGN OF 2-PORT HIGH GAIN MIMO ANTENNA

In order to make the array antenna with high gain and low sidelobe have the function of MIMO transceiver integration, the array antenna designed in the previous section is combined into a 2-port high gain MIMO antenna in this section. To reduce the mutual coupling between MIMO antennas, this article loads a hollow T-shaped branch in the middle of the ground plane. The size l_1 of the hollow T-shaped branch is calculated by Eq. (9). The function of the hollow T-shaped branch is to introduce the current between two MIMO antennas into the hollow T-shaped branch, thereby reduce the mutual coupling between MIMO antennas. The structure of the high gain MIMO antenna after further simulation optimization by CST is shown in Figure 11. Table 4 shows the final dimensions of the antenna obtained after simulation optimization.

$$l = \frac{c}{f\sqrt{2(\epsilon_r + 1)}} \tag{9}$$

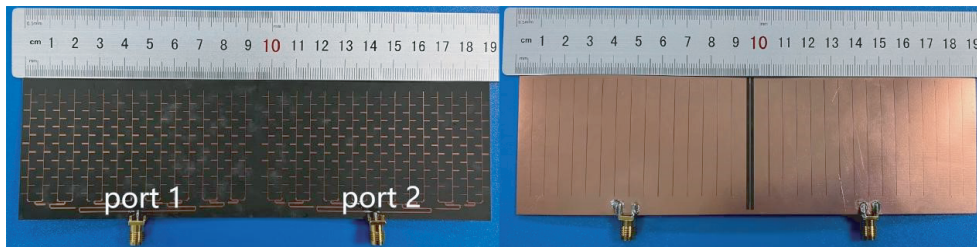
Table 4. Final size of antenna.

Parameters	Value/ mm	Parameters	Value/ mm	Parameters	Value/ mm	Parameters	Value/ mm
w_m	0.64	l_m	1.386	w_f	0.217	l_f	44.22
ss	3.058	l_s	2.66	w_1	0.213	w_2	0.276
w_3	0.374	w_4	0.493	w_5	0.605	w_6	0.685
w_7	0.714	w_8	0.685	w_9	0.605	w_{10}	0.493
w_{11}	0.374	w_{12}	0.276	w_{13}	0.213	W	190.46
L	56.65	l_1	3	l_2	54.65	l_3	49

**Figure 11.** MIMO antenna structure.

5. ANALYSIS OF SIMULATION AND MEASUREMENT RESULTS

The MIMO antenna was physically fabricated using the chemical etching method. In this section, the 2-port high gain MIMO antenna is physically tested, and the simulation results are compared and analyzed with the measured results. Figure 12 shows a photo of the antenna physical diagram, and Figure 13 shows a photo of the antenna testing site in a microwave anechoic chamber.

**Figure 12.** Antenna physical diagram.

5.1. S-Parameters

Figure 14 compares simulated and measured S -parameters of the high gain MIMO antenna. The simulated and measured resonant frequencies are around 39 GHz. The simulated and measured



Figure 13. Antenna testing site in a microwave anechoic chamber.

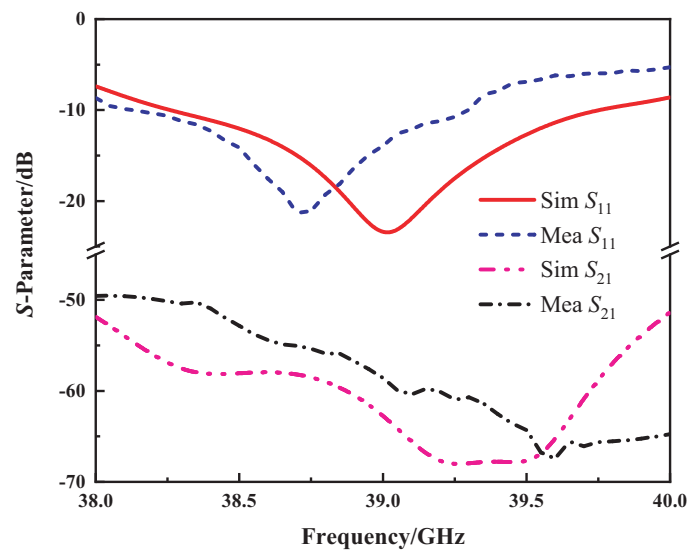


Figure 14. S -parameter simulation and measurement.

bandwidths are 38.2 ~ 39.7 GHz and 38.1 ~ 39.3 GHz, respectively, and S_{21} is below -50 dB. It shows that the antenna has a high degree of isolation, which meets the design requirements of the MIMO antenna and has outstanding advantages. Overall, the measurement results match the simulation ones but with slight differences. The reason for analyzing the error may be the loss generated by the soldering between the connector and the antenna, which affects the antenna's performance.

5.2. Gain and Efficiency

The gain and efficiency of the MIMO antenna are shown in Figure 15. It can be seen that the antenna gain reaches its maximum near 39 GHz with 26.2 dBi and 25.75 dBi for the simulated and measured gains, respectively. The measured results show that the antenna has a gain higher than 25 dBi in all the working bands, which reaches the design goal of 25 dBi and is entirely in line with the requirements of long-distance communication. Moreover, the antenna has high radiation efficiency, stabilizing at about 90% in the working frequency band.

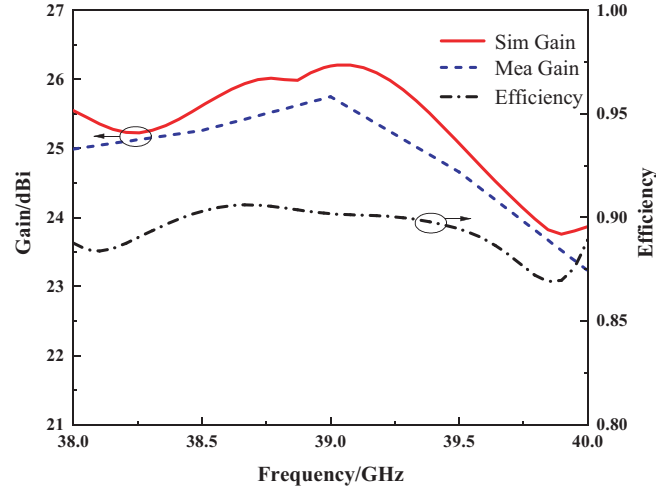


Figure 15. Gain and Efficiency.

5.3. Radiation Characteristics

The 39 GHz normalized radiation pattern is obtained when port 1 is excited, and Port 2 is loaded with a 50Ω matching load as shown in Figure 16. The simulated and measured sidelobe levels of the E -plane are -22.6 dB and -20.5 dB, respectively, and the simulated and measured sidelobe levels of the H -plane are -22 dB and -20 dB, respectively. The results show the consistency between the measured and simulated radiation patterns, and the MIMO antenna has strong directionality. Based on the radiation direction diagram, it can be concluded that this antenna can be applied to 5G millimeter wave outdoor point-to-point relay transmission to improve the transmission distance.

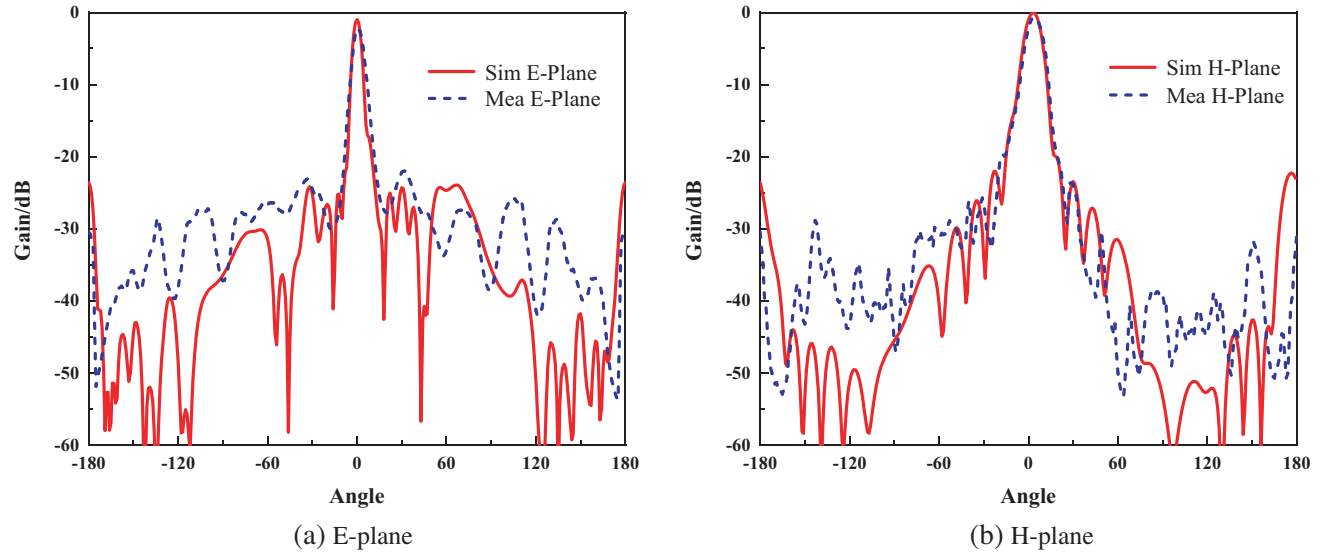


Figure 16. Normalized Radiation pattern.

5.4. ECC and DG

Envelope Correlation Coefficient (ECC) is an essential parameter of MIMO antenna that describes the degree of correlation between multiple antennas near each other. Another performance metric of MIMO is Diversity Gain (DG). The reduction in antenna transmission power only affects the quality

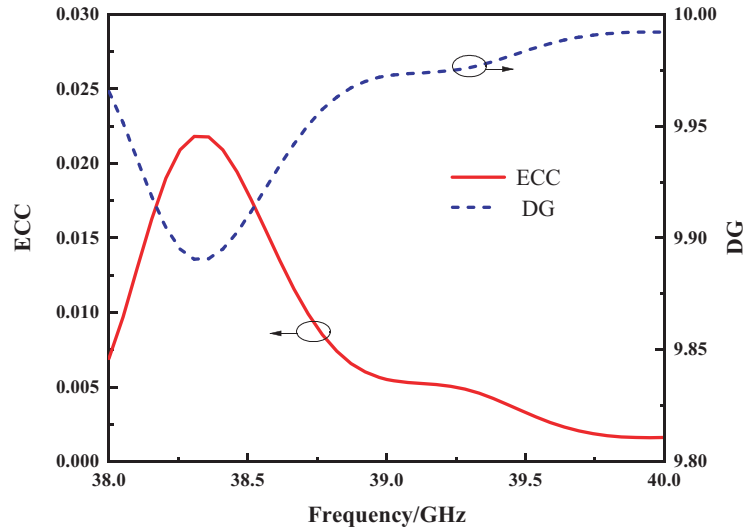


Figure 17. ECC and DG.

and performance of the MIMO transmissions if the DG is close to the standard value of 10. From Figure 17, It can be seen that the simulated ECC and DG values are less than 0.022 and greater than 9.89 in the whole frequency band, respectively; at 39 GHz, the ECC and DG values are 0.005 and 9.97, respectively, which satisfy the requirements of the MIMO antenna that the EEC value is less than 0.5 and DG close to 10. The results show that the designed antenna has good correlation performance, high independence, and meets the requirements of the MIMO antenna.

Table 5 shows the performance comparison of the high gain MIMO antenna designed in this paper with other high gain MIMO antennas and array antennas that also use the Taylor synthesis method for antenna design. Reference [18] describes a comb array antenna designed using the Taylor synthesis method with a gain of 24 dBi and sidelobe level of -13 dB. Compared with [18], the antenna designed in this paper has the advantage regarding gain and sidelobe level. The isolation is 5 dB higher than that in [19]; the gain and efficiency are 12.95 dBi and 5% higher than that in [14], respectively; the sidelobe level is 7.52 dB better than that in [20]. This comparison proves that the high gain MIMO antenna designed in this paper has the advantage of high gain and low sidelobe level and has outstanding comprehensive performance compared with similar antennas.

Table 5. Reference Comparison.

Reference	Frequency/ GHz	Port number	Isolation/dB	Gain/dBi	Efficiency	SLL/dB	ECC	DG
Ref. [18]	77	1	-	24	-	-13	-	-
Ref. [12]	28	4	-17	8.3	-	-	0.01	9.96
Ref. [13]	41	2	-28	9.86	84%	-	0.02	-
Ref. [14]	37	2	-40	12.8	85%	-11.7	0.00014	9.99
Ref. [19]	26	4	-45	10.27	-	-	0.0002	9.99
Ref. [20]	24 & 77	2	-25 & -44.26	11.8 & 8.34	-	-12.48 & -4	0.1	9.6
Ref. [21]	26	4	-23	7.25	-	-11.25	-	-
Ref. [22]	28 & 38	2	-20	8	80%	-10	0.0001	9.99
This paper	39	2	-50	25.75	90%	-20	0.005	9.97

6. CONCLUSION

In this paper, a 2-port high gain millimeter-wave MIMO antenna for 5G applications is designed with dimensions of $190.46 \times 56.65 \times 0.254 \text{ mm}^3$ and operating bandwidth of $38.1 \sim 39.3 \text{ GHz}$. A hollow T-shaped branch is introduced in the ground plane to make the antenna isolation more significant than 50 dB. The series-parallel hybrid feeding technique is adopted to increase the antenna's gain to 25.75 dBi at 39 GHz. The antenna sidelobe levels of -20.5 dB and -20 dB in the E -plane and H -plane are achieved with the help of Taylor synthesis and trenching techniques, respectively. Antenna gain more than 25 dBi and efficiency up to 90% can be achieved in the operating band. The maximum value of the envelope correlation coefficient (ECC) is 0.022, which is much smaller than 0.5; the diversity gain (DG) is close to 10; and the minimum value is 9.89. Based on the simulation and measurement results analysis, the high gain and low sidelobe level MIMO antenna designed in this paper can be applied in 5G millimeter-wave outdoor long-range point-to-point wireless relay communication system.

7. DATA AVAILABILITY

The datasets used and analysed during the current study are available from the corresponding author on reasonable request.

ACKNOWLEDGMENT

1. Liaoning Applied Basic Research Program (2022JH2/101300275).
2. National Fund: Research on Power Amplifier Design Modeling and Predistortion of Cognitive Radio System under Compressed Sensing Framework (61701211).
3. General Program of National Natural Science Foundation of China: Research on Modeling of Future-Oriented Reconfigurable Radio Frequency Module and Neural Network (61971210).
4. Horizontal project of Liaoning Technical University: Development of RF module automatic test system (23-2143).

REFERENCES

1. Raheel, K., A. Altaf, A. Waheed, S. H. Kiani, D. A. Sehrai, F. Tubbal, and R. Raad, "E-shaped H-slotted dual band mmWave antenna for 5G technology," *Electronics*, Vol. 10, No. 1, 1019, 2021.
2. Zhu, X., "Study on the propagation characteristics of outdoor microcell millimeter wave 39 GHz," Nanjing University of Posts And Telecommunications, 2018.
3. Yang, T. and X. Yuan, and I. B. Collings, "Reduced-dimension cooperative precoding for MIMO two-way relay channels," *IEEE Transactions on Wireless Communications*, Vol. 11, No. 11, 4150–4160, 2012.
4. Xu, S. and Y. Hua, "Optimal design of spatial source-and-relay matrices for a non-regenerative two-way MIMO relay system," *IEEE Transactions on Wireless Communications*, Vol. 10, No. 5, 1645–1655, 2011.
5. Vaze, R. and R. W. Heath, "On the capacity and diversity-multiplexing tradeoff of the two-way relay channel," *IEEE Transactions on Information Theory*, Vol. 57, No. 5, 4219–4234, 2011.
6. Gao, M. M., Y. Song, J. C. Nan, et al., "Research of a compact UWB-MIMO antenna with X band-rejected," *Journal of Electronic Measurement and Instrumentation*, Vol. 36, No. 1, 149–156, 2022.
7. Nan, J. C., X. X. Han, M. M. Gao, et al., "Design of miniaturized UWB-MIMO antenna based on DGS," *Journal of Electronic Measurement and Instrumentation*, Vol. 36, No. 5, 89–95, 2022.
8. Ali, W., S. Das, H. Medkour, et al., "Planar dual-band 27/39 GHz millimeter-wave MIMO antenna for 5G applications," *Microsystem Technologies*, Vol. 27, No. 1, 283–292, 2021.

9. Ali, M., L. E. G. Muñoz, G. Carpintero, S. Nellen, and B. Globisch, "Millimetre-wave photonic emitter integrating a PIN-PD and planar high gain antenna," *Proceedings of the IEEE Third International Workshop on Mobile Terahertz Systems (IWMTS)*, 1–5, Essen, Germany, July 2020.
10. Gao, F. L., J. Feng, C. Liao, et al., "Design of planar antenna array with broad beamwidth at 24 GHz," *Electronic Measurement Technology*, Vol. 42, No. 1, 112–115, 2019.
11. Li, Y. J., H. Sun, X. X. Yang, et al., "28 GHz microstrip array antenna with CSRR," *Electronic Measurement Technology*, Vol. 41, No. 18, 80–84, 2018.
12. Khalid, M., S. I. Naqvi, N. Hussain, et al., "4-port MIMO antenna with defected ground structure for 5G millimeter wave applications," *Electronics*, Vol. 9, No. 1, 71, 2020.
13. Manan, A., S. I. Naqvi, M. A. Azam, et al., "MIMO antenna array for mm-wave 5G smart devices," *2019 22nd International Multitopic Conference (INMIC)*, 1–5, Islamabad, Pakistan, 2019.
14. Khan, J., S. Ullah, U. Ali, et al., "Design of a millimeter-wave MIMO antenna array for 5G communication terminals," *Sensors*, Vol. 22, No. 7, 2768, 2022.
15. Wu, D., "76–81 GHz planar antenna development and utilization for automotive radar applications," M.S. Thesis, Department of Microtechnology and Nanoscience, Chalmers University of Technology, Gothenburg, Sweden, 2016.
16. Wang, J., Y. N. Zheng, and Z. Y. He, *Antenna Array Theory and Engineering Applications*, Publishing House of Electronics Industry, Beijing, 2015.
17. Zhang, L., W. Zhang, and Y. P. Zhang, "Microstrip grid and comb array antennas," *IEEE Transactions on Antennas and Propagation*, Vol. 59, No. 11, 4077–4084, 2011.
18. Zhang, Q., L. Wang, and X. Zhang, "Millimeter-wave microstrip comb-line antenna array for automotive radar," *2018 12th International Symposium on Antennas, Propagation and EM Theory (ISAPE)*, 1–3, Hangzhou, China, December 2018.
19. Tariq, S., S. I. Naqvi, N. Hussain, et al., "A metasurface-based MIMO antenna for 5G millimeter-wave applications," *IEEE Access*, Vol. 9, 51805–51817, 2021.
20. Subitha, D., S. Velmurugan, M. V. Lakshmi, et al., "Development of Rogers RT/Duroid 5880 substrate-based MIMO antenna array for automotive radar applications," *Advances in Materials Science and Engineering*, Vol. 2022, 4319549, 2022.
21. Zhou, X., H. Zhai, L. Xi, et al., "A low-profile four-element MIMO antenna array with new decoupling structures," *Microwave and Optical Technology Letters*, Vol. 60, No. 10, 2511–2516, 2018.
22. Tsao, Y. F., A. Desai, and H. T. Hsu, "Dual-band and dual-polarization CPW Fed MIMO antenna for fifth-generation mobile communications technology at 28 and 38 GHz," *IEEE Access*, Vol. 10, 46853–46863, 2022.